

The motion of single immiscible drops through a liquid

By R. SATAPATHY

Shri Ram Institute for Industrial Research, Delhi

AND W. SMITH

D.S.I.R. Warren Spring Laboratory, Stevenage, Herts.

(Received 21 October 1960)

The motion of drops of liquid through an immiscible field liquid has been observed and drag coefficients have been measured at Reynolds numbers from 0.01 to 1500. Several kinds of motion have been distinguished and it has been noticed that a change in the motion is always preceded by an increase in the drag coefficient and is usually followed by a return to the drag coefficient for solid spheres. When the drop is deformed, the drag coefficient and the form of the motion is not determined solely by the Reynolds number. The effect of the walls of a containing vessel on the motion is computed for low Reynolds numbers.

Introduction

Bringing into contact two immiscible phases and transferring a mutually soluble component from one phase to the other is a process frequently encountered in the chemical industry. Usually, one phase is dispersed in the other in the form of bubbles of gas or vapour, drops of liquid or particles of solid in such a way as to give a high interfacial area and a good rate of mass or heat transfer. The mechanics of the motion of the dispersed phase through the continuous phase is important in all these cases for two reasons: first, the velocity of the particles of the dispersed phase determines the capacity of the equipment; and secondly, the motion near the interface between the phases determines the convective rate of transfer of mass or heat between the particles and the continuous phase.

The capacity of industrial equipment can be related to the terminal velocity of single particles in an extended fluid. The terminal velocity (or drag coefficient) of single particles of solid or bubbles of gas has been measured by many workers, but liquid drops have until recently received less attention (Hughes & Gilliland 1952; Hu & Kintner 1955; Licht & Narasimhamurty 1955; Klee & Treybal 1956; Krishna, Venkateswarlu & Narasimhamurty 1959; Warshay, Bogusz, Johnson & Kintner 1959). These, like gas bubbles, have a more complicated motion than solids, for they are able to deform and oscillate, and owing to the difficulty of obtaining accurate data there is some conflict between the measurements of different workers. Although the scatter in values of drag coefficient is small, there is uncertainty about those values of the Reynolds number at which the character of bubble motion changes; for instance, when oscillation starts, or when vortices

are detached. As will be shown, under conditions where the drop is deformed, changes in the state of the motion are not decided by the value of the Reynolds number alone. It is important to know what kind of motion the drop has for this critically affects the rate of mass or heat transfer between the phases. For this reason careful measurements were made, during this work, of the drag coefficient of drops of liquid as a function of Reynolds number, and these values were correlated with the kind of motion observed.

Experimental equipment used for solvent extraction is often designed to give a long contact time between the two liquids and the Reynolds number of drops moving through the equipment is therefore low. The drops are sometimes in viscous flow (Stokes region) or move with a stable single-ring vortex at the rear; that is, below the Reynolds number at which vortices detach or at which there is much deformation. This region especially has been examined and the effect of containing walls on the motion has been calculated approximately. Also, since at low Reynolds numbers accurate measurements can be compared with theory, it is possible to decide whether the surface viscosity of Boussinesq (1913) plays an important part in determining the motion of the drop. Surface viscosity has been invoked recently to explain several phenomena noticed in liquid-liquid extraction (Sterling & Scriven 1959).

Experimental technique

The drag coefficient is given by

$$C_D = \frac{W}{\frac{1}{2}\rho U^2 \pi a^2}. \quad (1)$$

U , the steady terminal velocity of the drop, is measured directly; W , the effective weight of the drop in the field liquid, is found from the volume of the drop; and a is the apparent radius of the drop as seen from the direction of its motion.

Photographs were taken by a ciné-camera of drops moving (usually falling) through a square column of 6 in. side and filled with the field liquid to a height of 6 ft. Drops were formed and released beneath the surface of the field liquid from nozzles with a straight bore and a flat face. Several sizes of nozzle were used to give a range of drop sizes. The nozzle was fed with drop liquid from a container giving a constant head at the tip of the nozzle. In this way, as the photographs showed, drops of constant size were obtained and at a fixed frequency. The interval between drops was regulated to be long enough for the disturbance of the field liquid by the previous drop to have decayed. The velocity of the drop was determined either from the ciné-film, that is, from the position of the drop in successive frames, or by measuring with a stop-watch the time taken by the drop to move through a height of 70 cm. Each result registered was the average of 20 determinations. It was found that a distance of about 50 cm was sufficient to allow all drops to attain their steady velocity, and all readings were taken at least 70 cm from the nozzle. All drops had a diameter less than 1 cm: at this ratio of container to drop size (about 15 to 1) the effect of the walls of the container on the terminal velocity of the drop is small (Uno & Kintner 1956). The volume of liquid accumulated at the end of the column by about 20 of the

same drops was measured; this gave the volume of each drop. The projected area of the drops as seen from the direction of their motion was measured from the photographs, assuming that the drops have a circular cross-section in a horizontal plane. The drop and field liquids were mutually saturated with each other in order to eliminate mass transfer between the phases during the experiments. The viscosity and density of the mutually saturated liquids were measured and these were used in all calculations.

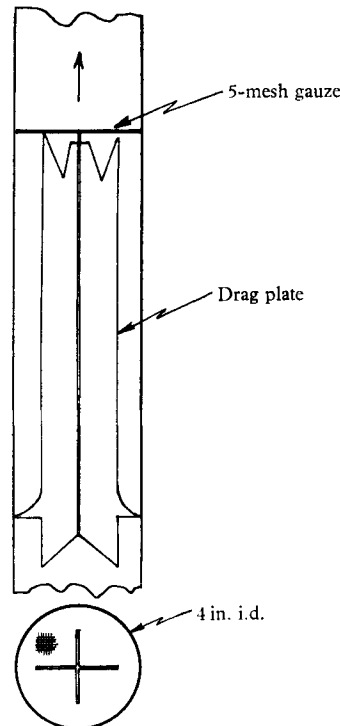


FIGURE 1. Drag plate.

At Reynolds numbers less than 40 the terminal velocity of solid spheres was measured in the same way as described above, except that the sphere was released from a hemispherical cup, to which it was initially attached by vacuum. The main purpose of these measurements was to check the experimental technique, and in the Stokes region ($R < 1$), the measured drag coefficient was within $\frac{1}{4}\%$ of the theoretical value, $24/R$ ($R = \rho U d / \mu$, ρ and μ being the density and viscosity of the field liquid, d being the maximum diameter of the drop in a horizontal plane).

Some experiments were carried out in which aluminium particles were added to the drop liquid, or dyestuff soluble in the field liquid was injected near the surface of the drop. This served to show up circulation of liquid within the drop or the vortex at the rear of the drop.

An apparatus was built in which it was possible to keep a drop stationary in a moving field liquid. This was effected by 'inverting' the velocity profile of the field liquid by placing a solid surface, a cruciform drag plate, along the axis

of the containing column and smoothing the disturbance so caused by a wire mesh (figure 1). It was possible by this means to keep the drop in the same horizontal plane in the centre of the column, and to observe oscillation of the drop or circulation within the drop. But quantitative measurement of the position of streamlines, shown up by injecting dyestuff in fine streams, was not accurate owing to uncertainty about the distribution of velocity in the liquid outside the drop. An alternative way of suspending the drops is to pass the field fluid vertically through a divergent conduit. This technique was used by Garner & Kendrick (1959) for suspending liquid drops in a gas stream, but was found here to be unsuitable for suspending liquid drops in a liquid.

Drag coefficient and drop motion

Drag coefficients, calculated by using equation (1), are plotted in figure 2 as a function of the Reynolds number. Glycerol, water and glycerol-water solutions (85, 65, 50 and 35 % by weight) were used as field liquids: these and the liquids forming the drops were all Newtonian in behaviour. Figure 2 is divided according to differences observed in the motion of the drops, which were as follows.

A. R less than 4

This is the viscous flow or Stokes region: the drops appear to be spherical and move steadily along a vertical straight line. At low Reynolds numbers (less than about 1) the streamlines at the front and rear of the drop appear to be distributed symmetrically. As the Reynolds number approaches 4 streamlines at the rear of the drop diverge, but no vortex is formed. The results shown are for drops having a size much greater than the critical value of Bond (1927, 1928); that is, liquid within the drop circulates in a symmetrical, stable ring vortex. Small drops which move as if they are solid spheres have been extensively studied before (Garner & Haycock 1959) and were not examined here. In order to obtain a low Reynolds number with a drop of a diameter of about $\frac{1}{2}$ cm, the field liquid must be very viscous (pure glycerol). Consequently most of the results plotted are close to the theoretical line predicted by Hadamard (1911) for the case where the viscosity of the drop liquid is zero ($16/R$).

B. R from 4 to 10

Above a Reynolds number of 4 the drag coefficient is higher than is predicted by Hadamard, and at a Reynolds number of 10 the drag coefficient attains the same value as is measured for solid spheres. A single-ring vortex, moving with the drop, forms at the rear; the stagnation point, that is the point where the outer boundary of this vortex returns to the axis of the motion, first moving from the drop at a Reynolds number of 4. At a Reynolds number of 10 the vortex has a total width of about $\frac{3}{4}$ of the diameter of the drop. Below a Reynolds number of 8 there is little deformation of the drop, but above a Reynolds number of 8 the rear of the drop progressively becomes flatter (figure 3). Inside the drop the liquid circulates, the centre of this motion appearing to move towards the front of the drop as the Reynolds number increases.

C. R from 10 to 45

As may be seen from figure 2 there appears to be a discontinuity in the slope of the curve of drag coefficient against Reynolds number at a Reynolds number of 10, and at Reynolds numbers between 10 and 40 the drag coefficient has the value found for solid spheres. As the Reynolds number approaches 40, the deformation of the drop becomes more pronounced and the vortex at the rear

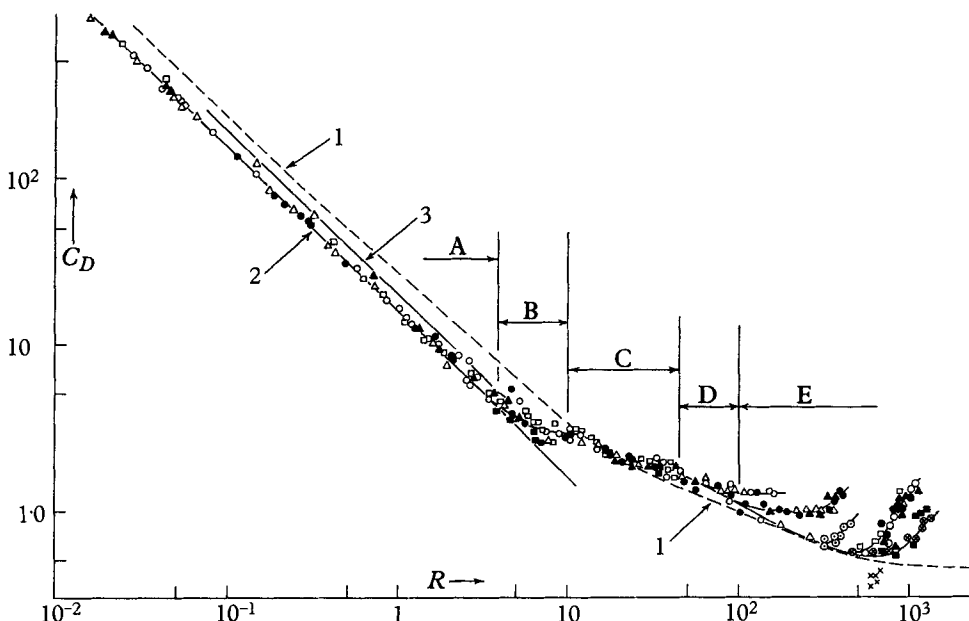


FIGURE 2. Drag coefficients. 1, solid spheres; 2, Hadamard ($\sigma = \infty$); 3, $\sigma = 7.5$. Experimental: \circ , tetrachloroethylene; \bullet , carbon tetrachloride; \triangle , chloroform; \blacktriangle , bromobenzene; \square , ethyl bromide; \blacksquare , carbon disulphide; \otimes , chlorobenzene; \odot , benzyl alcohol; \times , aniline.

suddenly increases in length, but never has a width greater than the equatorial diameter of the drop (figure 3). The way in which liquid within the drop moves becomes complicated and difficult to observe. Above a Reynolds number of 40 the drop moves unsteadily; the vortex stays attached to the rear of the drop, but attains its maximum size and moves from side to side about the axis of the motion. Between Reynolds numbers of 40 and 45 the drag coefficient is higher than the value measured for solid spheres.

D. R from 45 to 100

The vortex at the rear of the drop begins to break up once the Reynolds number is greater than 45. In turn each side of the vortex grows in size, the other side remaining small and stable, until it is greater in length than about $1\frac{1}{2}$ drop diameters when a part of the elongated vortex detaches itself (figure 3). The drop is deformed but again moves steadily, the drag coefficient remaining a little higher than the value measured for solid spheres. There appears to be little or no internal circulation.

E. *R* greater than 100

In this region vortices are detached from alternate sides of the drop, as described above, but the drop no longer moves steadily. In some cases the drop fluctuates in shape as shown in figure 3, while in other cases there is no axial symmetry in the shape of the drop. Circulation of liquid inside the drop appears to stop when oscillation of the surface commences. Above a Reynolds number of 300 the drop no longer moves in a vertical plane but follows the line of a helical spiral: this

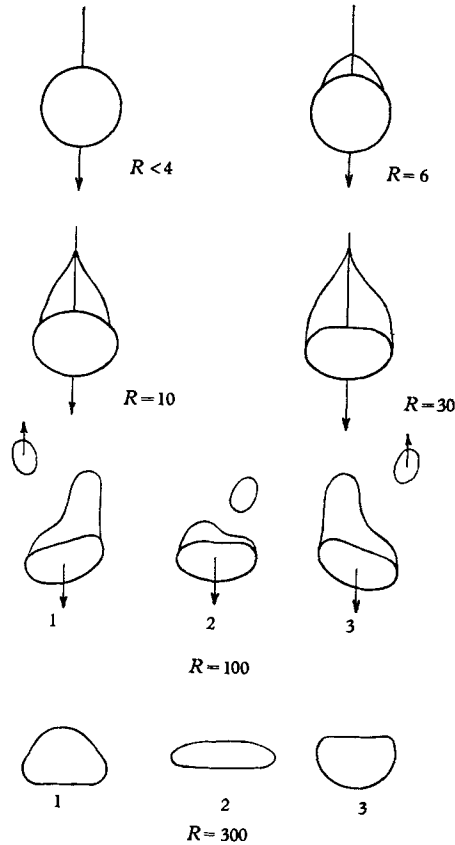


FIGURE 3. Drop shapes.

appears to be induced by the alternate detachment of vortices at the rear of the drop. Deviation from a vertical path is less with larger drops (see Margarvey & Bishop 1960). Drops formed from different liquids but moving in the same field liquid have different drag coefficients, the value (except for aniline) being greater than that for solid spheres. Evidently, under conditions where the surface of the drop is expanded and contracted, the drag coefficient will depend upon the interfacial tension (γ) as well as the Reynolds number. This is indicated by the fact that these results are correlated by the Weber number ($\rho U^2 a / \gamma$) by the method proposed by Hu & Kintner (1955). The various lines of the plot of drag coefficient against Reynolds number each terminate below a Reynolds number of 1500, at the condition where a drop breaks up before attaining a dynamically steady motion.

Analysis for low Reynolds numbers

In experimental equipment used to study mass transfer in solvent extraction processes, often single drops are allowed to move under the action of gravity in relatively narrow tubes and at low Reynolds numbers. The effect of the confining walls of the vessel on the position of the streamlines near the surface of the drop and on the drag coefficient can be calculated in the simple although approximate way suggested by Williams (1915): that is, by putting the disturbance caused by the drop as zero at a concentric spherical boundary moving with the drop. Less accurately, the influence on the motion of the presence of other drops can be estimated in the same way. It is possible to fit boundary conditions at a cylindrical surface coaxial with the axis of drop motion (Bohlin 1960), but this gives an answer which is too complicated for straightforward use.

Stokes's solution of the equations of motion in spherical polar co-ordinates for a viscous fluid is, in terms of the stream function,

$$\psi = (A/r + Br + Cr^2 + Dr^4) \sin^2 \theta; \tag{2}$$

r is the distance from the centre of the sphere and θ is the latitude. It is assumed that there is symmetry in planes through the axis of the motion. This solution can be used both for fluid outside and inside the drop (quantities referring only to the fluid inside the drop will be distinguished by primes). The component velocities are

$$u_r = \frac{1}{r^2 \sin \theta} \frac{\partial \psi}{\partial \theta}, \quad u_\theta = -\frac{1}{r \sin \theta} \frac{\partial \psi}{\partial r}. \tag{3}$$

All quantities are made dimensionless and are related to the dimensional quantities in terms of U , the steady terminal velocity and a , the radius of the drop. We apply the following boundary conditions which lead to the necessary number of relationships between the coefficients of r in equation (2).

(a) For a stationary drop with the field fluid moving at the outer, concentric, spherical boundary (of radius σ) at a dimensional velocity of U (or a dimensionless velocity of unity), we have

$$r = \sigma, \quad u_r = \cos \theta, \quad u_\theta = -\sin \theta.$$

This gives, by equations (3),

$$\frac{2A}{\sigma^3} + \frac{2B}{\sigma} + 2C + 2D\sigma^2 = 1, \tag{4}$$

$$-\frac{A}{\sigma^3} + \frac{B}{\sigma} + 2C + 4D\sigma^2 = 1. \tag{5}$$

(b) On the spherical surface of the stationary drop, since there is no deformation we must have the normal velocities of both fluids zero and the tangential velocities equal. For

$$r = 1, \quad u_r = u'_r = 0, \quad u_\theta = u'_\theta.$$

This leads to

$$A + B + C + D = 0, \tag{6}$$

$$A' + B' + C' + D' = 0, \tag{7}$$

$$A - B - 2C - 4D = A' - B' - 2C' - 4D'. \tag{8}$$

(c) The velocity of fluid inside the drop at $r = 0$ must remain finite, which dictates that

$$A' = B' = 0. \quad (9)$$

(d) At the surface of the drop the tangential stresses must be equal

$$r = 1, \quad p_{r\theta} = p'_{r\theta},$$

where

$$p_{r\theta} = \frac{2}{R} \left(\frac{\partial u_\theta}{\partial r} + \frac{1}{r} \frac{\partial u_r}{\partial \theta} - \frac{u_\theta}{r} \right).$$

This gives

$$(A' + D') = v(A + D), \quad (10)$$

where

$$v = \mu/\mu'.$$

Solution of equations (4) to (10) leads to

$$\begin{aligned} B &= -\frac{3\sigma^6 - 3\sigma + 2\sigma^6 v + 3\sigma v}{4\sigma^6 - 9\sigma^5 + 10\sigma^3 - 9\sigma + 4\sigma^6 v - 6\sigma^5 v + 6\sigma v + 4v}, \\ D &= \frac{2B\sigma^3 + 4B - 6B\sigma - 3\sigma}{4\sigma^6 - 10\sigma^3 + 6\sigma}, \\ C &= \frac{1}{2} - \frac{2B}{3\sigma} - \frac{5D\sigma^2}{3}. \end{aligned} \quad (11)$$

A is then given by equation (6), D' by equation (10) and C' by equation (7).

The total of the forces acting at the surface of the drop in the direction of its motion is the drag force, which in steady motion is equal to the effective weight of the drop. The drag coefficient is given by

$$C_D = 4 \int_0^\pi (p_{rr} \cos \theta - p_{r\theta} \sin \theta)_{r=1} \sin \theta d\theta, \quad (12)$$

where

$$p_{rr} = -p + \frac{4}{R} \frac{\partial u_r}{\partial r}, \quad (13)$$

and p is obtained from the equations of motion as a function of θ . Equations (12) and (13) give

$$C_D = -16 \frac{\mu}{\rho U a} B = -\frac{32}{R} B. \quad (14)$$

Equation (14) can also be obtained by finding the dissipation of energy by viscous motion of fluid inside and outside the drop. If the totals of the normal stresses on each side of the interface are calculated, it is now found that they are equal; that is, the sum of the dynamic pressure, hydrostatic head and viscous stress outside the drop equals the sum of the dynamic pressure, viscous stress and the normal stress owing to interfacial tension inside the drop.

Comparison with experiment

In equation (11), if σ is put equal to infinity, we get

$$B = -\frac{3}{4} \frac{2\mu + 3\mu'}{3\mu + 3\mu'}.$$

By equation (14), the drag coefficient is

$$C_D = \frac{24}{R} \frac{2\mu + 3\mu'}{3\mu + 3\mu'}. \quad (15)$$

This is Hadamard's solution. In our experiments σ had a high value of about 15. Even so, there is an appreciable difference between the drag coefficient given by equation (14) and that given by equation (15). For instance, for a drop of tetrachloro-ethylene ($\mu' = 0.00851$ poise) in 85% by weight glycerol ($\mu = 0.5495$ poise), when $\sigma = 15$, $B = -0.560$ and by equation (14), $C_D = 17.9/R$; and when $\sigma = 7.5$, $B = -0.631$ and $C_D = 20.2/R$ (see figure 2). By equation (15) Hadamard's solution gives for the same liquids $C_D = 16.1/R$.

The maximum velocity at which fluid moves inside the drop (V_c) occurs at the origin along the axis of motion, and this is the same in magnitude as the tangential velocity at the surface at the equator of the drop. By equations (2) and (3)

$$V_c = -2C'.$$

For the liquids considered above and for $\sigma = 15$, $C' = -0.258$. So $V_c = +0.516$; that is, 52% of the velocity with which the drop is moving. An internal circulation of this magnitude should be readily observable even in small drops. But the observation of Bond (1927) (and more recently of Garner & Haycock 1959) is that there is a specific size of drop below which there is no circulation. Thus, with small drops there must be tangential stresses other than the viscous stress which restrict the transmission of motion from the field to the drop liquid.

According to Boussinesq (1913) the dynamic value of interfacial tension is different from the static value (γ). In dimensionless terms the difference in normal stress is

$$2 \left[\frac{1}{We} + \frac{1}{R_s} \left(\frac{\partial u_\theta}{\partial \theta} \right)_{r=1} \right],$$

and in tangential stress is $(u_\theta/R_s)_{r=1}$, where $R_s = \rho U a^2 / \mu_s$ and μ_s is called the surface viscosity. Applying these relations, in the normal stress the first term ($2/We$) merely increases the mean normal pressure inside the drop by the static value of the interfacial tension and has no effect on the solution. If the remaining terms owing to surface viscosity are accounted for we find, after Boussinesq,

$$C_D = \frac{24}{R} \left(\frac{2\mu + 3\mu' + e}{3\mu + 3\mu' + e} \right), \quad (16)$$

for $\sigma = \infty$. The experimental results obey equation (15) rather than equation (16) and show that the surface viscosity is small.

We should like to thank Professor D. M. Newitt for his guidance and for providing facilities for this work, which was done at the Department of Chemical Engineering, Imperial College. One of the authors (R. S.) wishes to acknowledge the award of the Assam Oil Co. scholarship.

REFERENCES

- BOHLIN, T. 1960 *Trans. Roy. Inst. Tech., Stockholm*, no. 155.
 BOND, W. N. 1927 *Phil. Mag.* **4**, 889.
 BOND, W. N. & NEWTON, D. R. 1928 *Phil. Mag.* **5**, 794.
 BOUSSINESQ, J. 1913 *Ann. Chem. Phys.* **29**, 349.
 GARNER, F. H. & HAYCOCK, P. J. 1959 *Proc. Roy. Soc. A*, **252**, 457.
 GARNER, F. H. & KENDRICK, P. 1959 *Trans. Inst. Chem. Engrs*, **37**, 155.

- HADAMARD, J. 1911 *C.R. Acad. Sci., Paris*, **152**, 1735.
- HU, S. & KINTNER, R. C. 1955 *J. Amer. Inst. Chem. Engrs*, **1**, 42.
- HUGHES, R. R. & GILLILAND, E. R. 1952 *Chem. Engng Prog.* **48**, 497.
- KLEE, A. J. & TREYBAL, R. E. 1956 *J. Amer. Inst. Chem. Engrs*, **2**, 444.
- KRISHNA, P. M., VENKATESWARLU, D. & NARASIMHAMURTY, G. S. R. 1959 *J. Chem. Engng Data*, **4**, 336.
- LICHT, W. & NARASIMHAMURTY, G. S. R. 1955 *J. Amer. Inst. Chem. Engrs*, **1**, 366.
- MARGARVEY, R. H. & BISHOP, R. L. 1960 *Nature, Lond.*, **188**, 735.
- STERNLING, C. V. & SCRIVEN, L. E. 1959 *J. Amer. Inst. Chem. Engrs*, **5**, 514.
- UNO, S. & KINTNER, R. C. 1956 *J. Amer. Inst. Chem. Engrs*, **2**, 420.
- WARSHAY, M., BOGUSZ, E., JOHNSON, M. & KINTNER, R. C. 1959 *Canad. J. Chem. Engng*, **37**, 29.
- WILLIAMS, W. E. 1915 *Phil. Mag.* **29**, 526.